

# Multi-GeV Electron Acceleration in Wakefields Strongly Driven by Oversized Laser Spots

K. Pöder<sup>1,2,\*</sup>, J. C. Wood<sup>1</sup>, N. C. Lopes<sup>1,3</sup>, J. M. Cole<sup>1</sup>, S. Alatabi,<sup>1</sup> M. P. Backhouse,<sup>1</sup> P. S. Foster,<sup>4</sup> A. J. Hughes,<sup>1</sup> C. Kamperidis<sup>1,5</sup>, O. Kononenko<sup>1,6</sup>, S. P. D. Mangles<sup>1</sup>, C. A. J. Palmer<sup>1,7</sup>, D. Rusby,<sup>4</sup> A. Sahai,<sup>1</sup> G. Sarri<sup>1,7</sup>, D. R. Symes,<sup>4</sup> J. R. Warwick,<sup>7</sup> and Z. Najmudin<sup>1,†</sup>

<sup>1</sup>The John Adams Institute for Accelerator Science, Imperial College, London SW7 2BZ, United Kingdom

<sup>2</sup>Deutsches Elektronen-Synchrotron DESY, D-22607 Hamburg, Germany

<sup>3</sup>GoLP/Instituto de Plasmas e Fusão Nuclear, Instituto Superior Técnico, Universidade de Lisboa, 1049-001 Lisbon, Portugal

<sup>4</sup>Central Laser Facility, Rutherford Appleton Laboratory, Didcot OX11 0QX, United Kingdom

<sup>5</sup>ELI-ALPS, ELI-HU Non-profit Ltd., Szeged, Hungary

<sup>6</sup>LOA, ENSTA ParisTech-CNRS-École Polytechnique-Université Paris-Saclay, 828 Boulevard des Maréchaux, 91762 Palaiseau Cedex, France

<sup>7</sup>Queen's University Belfast, Belfast, BT7 1NN, United Kingdom



(Received 19 October 2023; accepted 1 March 2024; published 10 May 2024)

Experiments were performed on laser wakefield acceleration in the highly nonlinear regime. With laser powers  $P < 250$  TW and using an initial spot size larger than the matched spot size for guiding, we were able to accelerate electrons to energies  $\mathcal{E}_{\max} > 2.5$  GeV, in fields exceeding  $500$  GV m $^{-1}$ , with more than  $80$  pC of charge at energies  $\mathcal{E} > 1$  GeV. Three-dimensional particle-in-cell simulations show that using an oversized spot delays injection, avoiding beam loss as the wakefield undergoes length oscillation. This enables injected electrons to remain in the regions of highest accelerating fields and leads to a doubling of energy gain as compared to results from using half the focal length with the same laser.

DOI: 10.1103/PhysRevLett.132.195001

Laser wakefield accelerators (LWFA) have become valuable tools in high-field science [1–3] and as drivers of particle [4] and radiation sources [5–7]. There are now many reports of acceleration of electrons to multi-GeV energies by LWFA [8–12]. But for many applications, it is desirable to have as high a charge of electrons at  $\sim$ GeV energies as possible [5,13–15].

The LWFA is a relativistic accelerating structure resulting from the space charge separation created by an intense laser pulse passing through an underdense plasma [16]. To attain the highest energies, the laser pulse must be guided over many Rayleigh lengths, which can be achieved by using plasma waveguides [10,12]. It is also common to use self-guiding [17–19], where diffraction of the laser pulse is balanced by the intensity-dependent response of the plasma refractive index. Self-guiding can occur for lasers exceeding a critical power  $P_{cr} = (2(4\pi\epsilon_0)m_e^2c^5/e^2)(\omega_0^2/\omega_p^2) \approx 17.4(n_{cr}/n_e)$  GW [20,21], where  $\omega_0$  is the laser frequency,  $\omega_p = (n_e e^2/c_0 m_e)^{1/2}$  is the plasma frequency, and  $n_{cr} = (\epsilon_0 m_e \omega_0^2)/e^2$  is the critical density.

The properties of the wakefield depend on the peak normalized vector potential of the laser,  $a_0 \equiv eE/m_e\omega_0c$ ,

where  $E$  is the electric field of the laser. At high intensity,  $a_0 \gtrsim 2$ , the maximum energy gain is given by [22]

$$\mathcal{E}_{\max} = \frac{2}{3}(\omega_0/\omega_p)^2 a_0 m_e c^2. \quad (1)$$

Simulations suggest that in this regime the laser can be self-guided at a matched size  $w_m = 2\sqrt{a_0}c/\omega_p$  [23]. In most experiments, the laser spot is initialized at close to  $w_m$  to ensure good guiding. Previous reports of multi-GeV acceleration using self-guided LWFA have required lasers exceeding PW powers [8,9,11].

In this Letter, we show that initiating the laser with an overly large spot, relative to  $w_m$ , leads to maximum energies of more than 2.5 GeV in electric fields exceeding 500 GV m $^{-1}$  with a laser power of only  $P = 230$  TW. This energy gain is more than double that which has been previously achieved in numerous experiments using the same laser system but with a smaller initial spot size [7,13,17,24,25]. The slower rate of self-focusing, and the concomitant reduction in spot width and  $a_0$  variations, reduces beam loss of injected electrons that can occur due to rapid variations in bubble length at early times. Electrons injected into the extreme fields at the back of the bubble remain focused and are rapidly accelerated to high energies.

The experiments were carried out using the Gemini laser at the Rutherford Appleton Laboratory, which provides linearly polarized laser pulses of central wavelength  $\lambda_0 = 800$  nm and pulse lengths down to  $\tau = (43 + 5)$  fs

Published by the American Physical Society under the terms of the Creative Commons Attribution 4.0 International license. Further distribution of this work must maintain attribution to the author(s) and the published article's title, journal citation, and DOI.

(FWHM). Using a folded focusing geometry (see Supplemental Material [36] for schematic), pulses of up to  $E_L = 11$  J ( $P \approx 230$  TW) were focused with a  $f = 6$  m spherical mirror ( $f/40$ ). A deformable mirror before the focusing optic corrected wavefront aberrations, allowing focusing to an elliptical spot with  $1/e^2$  intensity (major, minor) radii of  $(w_{\text{major}}, w_{\text{minor}}) = (48 \pm 2, 37 \pm 2)$   $\mu\text{m}$ . The peak vacuum intensity for  $E_L = 11$  J on target was  $I_0 = (6.8 \pm 0.9) \times 10^{18}$  W cm $^2$ , ( $a_0 = 1.8 \pm 0.1$ ).

The laser was focused on the entrance of a helium gas cell of length variable from  $L = 3$  to 42 mm. The plasma density was characterized by transverse moiré interferometry [26], resulting in an error of 12%. The generated electron beam was measured with a permanent magnet dipole spectrometer with  $B_{\text{peak}} = 0.95$  T over a length of  $l_B = 42$  cm and its field set perpendicular to the laser polarization. The deflected electrons were detected on two phosphor screens (Lanex regular) imaged on to 16-bit CCD cameras, allowing the energy of the electron beam to be determined with no ambiguity due to pointing variations [27,28]. Typically one common feature in the high-energy part of the electron was used for backtracking (example in Supplemental Material).

Single-shot images from the spectrometer are shown in Fig. 1, highlighting three different acceleration regimes that could be accessed by varying operating parameters. At the lowest densities at which electron beams were detected, typically  $n_e \simeq 1.6 \times 10^{18}$  cm $^{-3}$ , narrow energy spread features could be produced, as shown in Fig. 1(a). This is atypical for self-guided self-injection experiments performed for laser powers  $P \simeq 200$  TW in uniform density targets, where multiple or even continuous injection is observed as beams are accelerated to high energy [17]. Beam charges up to 4 pC were produced in FWHM energy spreads as low as 4%. These features were sensitive to laser and plasma parameters but interestingly were persistent for increases in plasma length.

Increasing laser energy increased the spectral brightness of the electron beam, but was accompanied by an increasing tail of low-energy electrons, as exemplified in Fig. 1(b). This beam features a high energy peak of about 20 pC in a 10% FWHM energy spread at a central energy  $\mathcal{E} = (1.39 \pm 0.02)$  GeV. At higher plasma density, a further increase in maximum energy was observed, but now in a beam with broad energy spread, as shown in Fig. 1(c). A maximum energy, defined as the energy where the signal rises to 5 times the standard deviation of noise at the high energy end of the spectrometer, of  $\mathcal{E}_{\text{max}} = (2.7 \pm 0.1)$  GeV was obtained at  $n_e = 2.9 \times 10^{18}$  cm $^{-3}$ . For this spectrum, the total beam charge was  $Q_{\text{tot}} \simeq 370$  pC, corresponding to more than 0.34 J. The charge exceeding 1 GeV was  $Q_{\mathcal{E}>1\text{ GeV}} = (100 \pm 2)$  pC, with the charge exceeding 2 GeV measured to be  $Q_{\mathcal{E}>2\text{ GeV}} = (17 \pm 1)$  pC.

The stability of the generated multi-GeV electron beams is presented in Fig. 2. Average spectra along with their

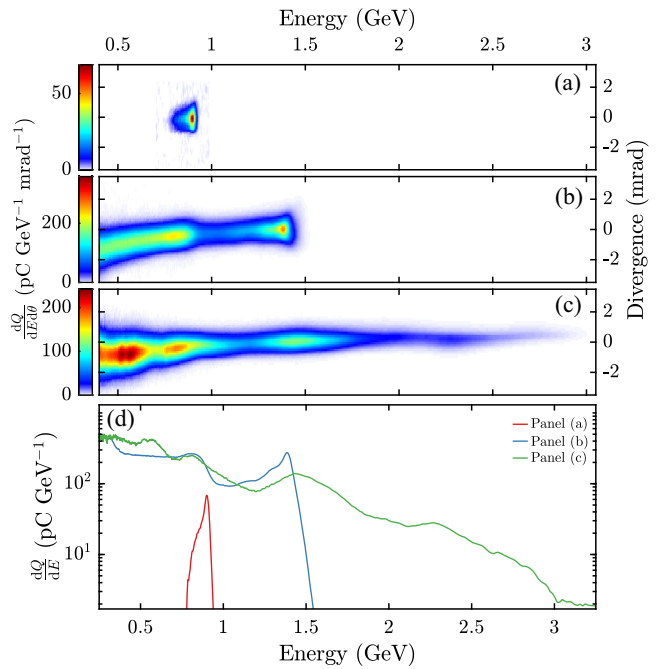


FIG. 1. (a)–(c) Sample electron spectrometer images: (a) narrow energy spread beam with  $\mathcal{E} = (0.90 \pm 0.01)$  GeV and FWHM energy spread  $\Delta\mathcal{E}/\mathcal{E} = 4\%$ , for  $(P, L, n_e) = (215$  TW, 32 mm,  $1.6 \times 10^{18}$  cm $^{-3}$ ); (b) beam with peak at  $\mathcal{E} = 1.4$  GeV and  $\Delta\mathcal{E}/\mathcal{E} = 10\%$ , for  $(240$  TW, 20 mm,  $1.6 \times 10^{18}$  cm $^{-3}$ ); (c) multi-GeV electron beam, with cutoff at  $\mathcal{E}_{\text{max}} = 2.7$  GeV for  $(240$  TW, 20 mm,  $2.9 \times 10^{18}$  cm $^{-3}$ ). Note the different color scales in (a)–(c). (d) spectra for (a)–(c).

standard deviation are plotted in Fig. 2(a) for  $P_L = 120$  TW and  $P_L = 240$  TW. Even with half the nominal laser energy ( $E_L = 5$  J), electron energies up to  $\mathcal{E}_{\text{max}} = (1.8 \pm 0.1)$  GeV and charges up to  $Q_{\text{tot}} \simeq 100$  pC were measured for  $n_e = 2.9 \times 10^{18}$  cm $^{-3}$  and  $L = 10$  mm. Thus, the energy gain was increased by at least 50% as compared to that obtained with twice the laser energy but with faster focusing [7,13,17,24,25].

The variation of the cut-off energy as a function of plasma length is shown in Fig. 2(b) for  $P_L = 120$  TW. The energy gain varies parabolically with acceleration length, as expected in the linearly varying fields of a cavitated plasma bubble [23]. Fitting a quadratic determines a peak field of  $E_{\text{peak}} = (360 \pm 30)$  GV m $^{-1}$  for  $n_e = 2.3 \times 10^{18}$  cm $^{-3}$  and  $E_{\text{peak}} = (570 \pm 190)$  GV m $^{-1}$  for  $n_e = 3.2 \times 10^{18}$  cm $^{-3}$ . These measurements highlight the extreme field strengths sampled by the electrons.

The scaling of cut-off energy and beam charge is plotted in Figs. 2(c) and 2(d) for fixed length  $L = 12.5$  mm and full laser power.  $\mathcal{E}_{\text{max}}$  is seen to increase with density and peaks at  $n_e \simeq 2.9 \times 10^{18}$  cm $^{-3}$ . The total beam charge,  $Q_{\text{tot}}$ , increases almost linearly with  $n_e$ , while the amount of high energy electrons ( $\mathcal{E} > 1$  GeV) is observed to also peak at  $n_e \simeq 2.9 \times 10^{18}$  cm $^{-3}$  with  $Q_{\mathcal{E}>1\text{ GeV}} = (80 \pm 7)$  pC.

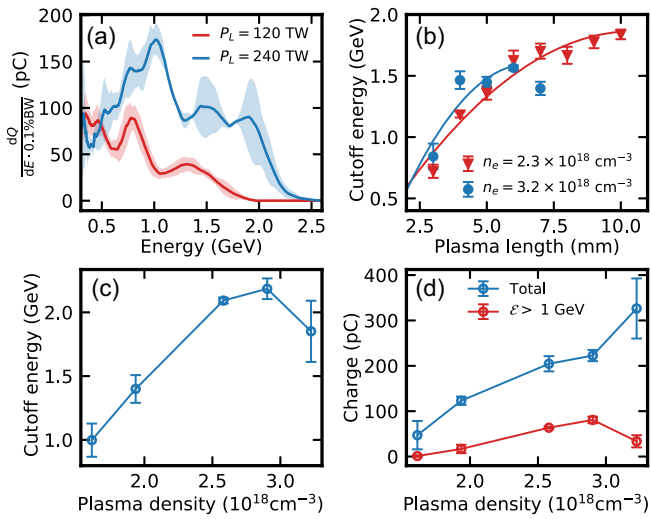


FIG. 2. (a) Average spectra (solid line) and standard deviation (highlighted area) of (red) 6 shots taken with  $(P, L, n_e) = (120 \text{ TW}, 10 \text{ mm}, 2.8 \times 10^{18} \text{ cm}^{-3})$  and (blue) 4 shots taken with  $(240 \text{ TW}, 12.5 \text{ mm}, 2.9 \times 10^{18} \text{ cm}^{-3})$ ; these represent all consecutively taken data for these conditions. (b) Variation of cut-off energy  $\varepsilon_{\max}$  with  $L$  at two different plasma densities for  $P = 120 \text{ TW}$ . The solid lines are parabolic fits to the data. Scaling of electron beam: (c)  $\varepsilon_{\max}$  and (d) beam charge with plasma density for  $L = 12.5 \text{ mm}$  and  $P = 240 \text{ TW}$ . The error bars in (c) and (d) are the standard deviation of the data points.

The maximum energies observed here are more than a factor of two greater than reported in numerous experiments using  $f/20$  focusing with the laser spot initiated close to  $2w_m$  [7,13,17,24,25]. This is surprising considering the lower initial intensity due to the  $f/40$  focusing. To gain further insight, quasi-3D particle-in-cell simulations were performed using FBPIC [29]. A linearly polarized laser pulse with  $\tau_{\text{FWHM}} = 43 \text{ fs}$  and a transverse Gaussian profile with  $w_0 = 42 \mu\text{m}$  was used to model the  $f/40$  focusing. For  $P = 120 \text{ TW}$ , this gives  $a_0 = 1.31$ . To model the  $f/20$  focusing, the laser power was kept constant by halving  $w_0$  and doubling  $a_0$ . The plasma profile consisted of a 0.5 mm linear ramp followed by a plateau of  $n_e = 2.3 \times 10^{18} \text{ cm}^{-3}$ . The laser was focused at the start of the plateau. The simulation box size was set to  $120 \times 120 \mu\text{m}$  in  $(x, r)$ . Three azimuthal ( $\phi$ ) modes were used with  $(2, 2, 6)$  particles per cell in  $(x, r, \phi)$ . The grid resolution was set to  $k_0 \Delta x = 0.2$  and  $k_p \Delta r = 0.04$  where  $k_0 = \omega_0/c$  is the laser and  $k_p = \omega_p/c$  is the wake wave number. The simulation box moved at the linear group velocity of the laser.

The electron energy spectrum evolution is shown in Figs. 3(a) and 3(b) for  $f/40$  and  $f/20$  focusing, respectively. The simulations reveal that the slower focusing produces higher energy gain, as observed experimentally. The increased energy gain can be understood by examining the variation of the peak  $a_0$  with propagation distance. While the  $a_0$  evolution is almost identical for both focusing

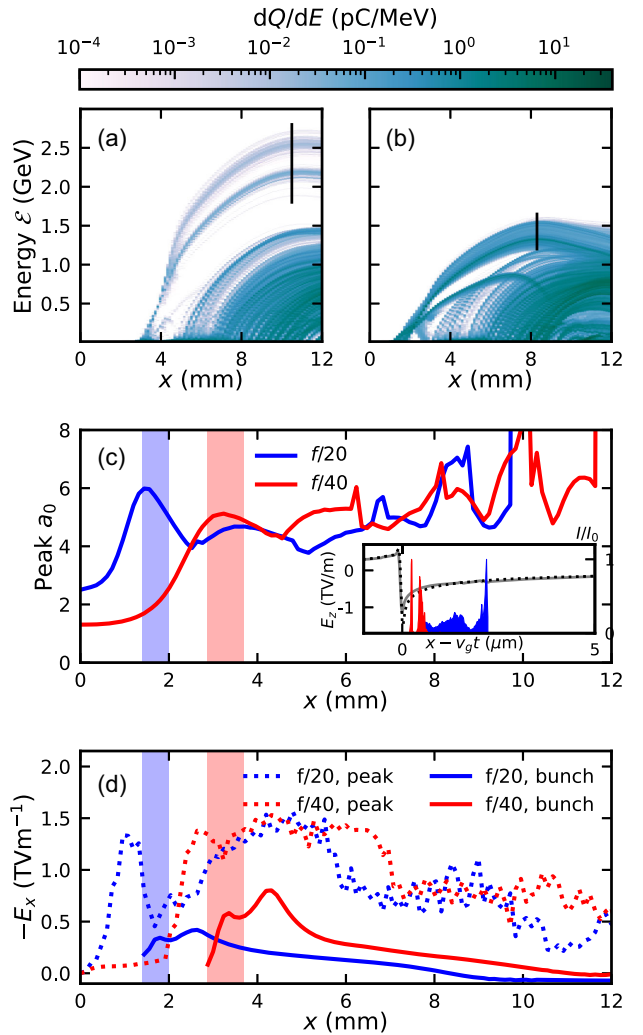


FIG. 3. Results from 3D particle-in-cell simulations: electron energy spectra as a function of propagation distance  $x$  for (a)  $f/40$  and (b)  $f/20$  focusing. (c)  $a_0$  as a function of  $x$  for  $f/20$  (blue) and  $f/40$  (red) simulations; inset shows the longitudinal profile of the wakefields ( $f/20$  in gray,  $f/40$  in black dots) and the independently normalized current profiles of the electron bunches in the moving window  $\sim 1 \text{ mm}$  after injection in both simulations. (d) peak longitudinal electric field in the bubble  $E_x$  (dotted lines) and the accelerating field experienced by electrons that reach the highest energies (solid lines). Electrons that gain the most energy are highlighted by solid vertical lines in panels (a) and (b), with their injection  $x$  positions highlighted by the shaded regions in (c) and (d).

geometries beyond 3 mm of propagation (Fig. 3(c)), there is a marked difference in the early-time behaviour. For the  $f/20$ , there is strong self-focusing for  $x < 1.5 \text{ mm}$ . The rapid increase in intensity leads to a lengthening of the plasma bubble, since  $\lambda_p = \sqrt{a_0}(2\pi c/\omega_p)$  [22], which stimulates self-injection [30]. The region over which the injection occurs is indicated in blue in Fig. 3(c). However, the laser focuses too strongly and diffraction starts to dominate, leading to a contraction in the bubble length

and loss of the electrons furthest in the back of the bubble. After  $x \approx 3$  mm, the diffraction leading to transverse expansion slows and the laser starts to self-focus again, leading to renewed bubble expansion followed by stable propagation. As electrons furthest at the back were lost due to bubble contraction, the accelerated electrons reside in an advanced phase and a lower acceleration gradient in the now larger bubble (see inset Fig. 3(c)).

For the  $f/40$ , self-focusing progresses more slowly, preventing electron injection until  $x \gtrsim 3$  mm [red region in Fig. 3(c)]. At this  $x$ , the pulse has a similar intensity profile to the  $f/20$  case. Consequently, the wakefield is almost identical in both cases [inset Fig. 3(c)]. However, for the  $f/40$  there was no rapid overfocusing and the injected electrons are therefore accelerated very close to the back of the accelerator cavity. As seen from Fig. 3(d), although the peak accelerating field for  $x > 3$  mm evolves similarly for both simulations, the injected electrons experience fields of nearly 800 GV/m in the  $f/40$  case. This value is almost double the fields experienced by the highest energy electrons in the  $f/20$  simulations. Note we see no self-steepening of the pulse in either simulation for  $x \approx 3$  mm, i.e., prior to injection. Therefore the observed differences are predominantly due to the self-focussing dynamics described above.

The difference in behavior between the two focussing geometries can be understood by considering the (first order) laser envelope equation  $d^2R/dx^2 = (1/z_R^2 R^3)(1-\alpha)$ , where  $R = w/w_0$  is the spot size normalized to the vacuum focal spot size,  $z_R = k_0 w_0^2/2$  is the Rayleigh range and  $\alpha = P/P_{\text{cr}}$  [31].  $d^2R/dx^2 < 0$  for  $\alpha \gg 1$ , leading to an increasing rate of compression of  $R$ . For a beam with  $dR/dx = 0$  at  $x = 0$ , an approximate solution is  $R^2 = 1 + (1-\alpha)(x/z_R)^2$  [32]. This predicts a rapid collapse of the pulse for  $x = z_R/\sqrt{\alpha} - 1$ . Full collapse is prevented by considering higher order terms to the envelope equation, especially plasma motion, which become important at small  $R$ . However, this equation gives a simple understanding of the behavior of the laser waist. For  $P = 120$  TW and  $n_e = 2.3 \times 10^{18}$  cm $^{-3}$ ,  $\alpha = 9.0$ , and spot collapse is expected at  $x \approx (0.7$  mm,  $2.5$  mm) for ( $f/20$ ,  $f/40$ ) focusing, respectively. Given the 0.5 mm ramps for both simulations, the highest intensity is reached at  $x \approx (1.3$  mm,  $3$  mm) for ( $f/20$ ,  $f/40$ ) focusing, matching the simulations well.

Previous 3D simulations in the nonlinear regime ( $a_0 \gtrsim 2$ ) have suggested that the matched spot size is given by  $k_p w_m \approx 2\sqrt{a_0}$  [22,23]. The factor of 2 was found to minimize oscillations in the transverse laser envelope, when the laser spot was initiated at close to this size. This is not applicable here, where the beam starts far from this value and evolves dynamically. Instead, the beam size reduces until the ponderomotive force on sheath electrons is balanced by the ion channel restoring force, giving  $k_p w_m = \sqrt{a_m}$ , thus omitting the factor 2. For constant

power, ( $a_0^2 w_0^2 = a_m^2 w_m^2$ ), the laser then self-focuses to  $w_m = (a_0 w_0 / k_p^2)^{1/3}$ , with a corresponding  $a_m = (a_0 w_0 k_p)^{2/3}$ . A similar scaling was obtained in Ref. [33]. The model predicts  $w_m \approx 9$  μm with  $a_m \approx 6$  for our simulations, reproducing the values observed in the simulations at the first spot size minimum for the  $f/20$ . The  $f/40$  does not focus so strongly. The longer time to the first self-focusing peak means the laser depletes enough to cause a small reduction in intensity at the focus,  $a_m \approx 5$ . Because of the weak dependence of  $w_m$  on power, though, it focuses to much the same size. Since the matched size is approached more gradually in this case, there is less subsequent expansion due to overfocusing. This more adiabatic approach to the matched spot size, minimizes bubble length variation which, as noted before, reduces loss of accelerating electrons.

Using the above considerations, we expect  $a_m \approx 6.4$  and  $a_m \approx 8.1$  for the half and full-energy shots, respectively. These are less than the  $a_{5J} \approx 9.3$  and  $a_{10J} \approx 10.3$  inferred from the measured cut-off energies of beams shown in Fig. 2 using Eq. (1). The discrepancy can arise from the idealized temporal pulse used in the simulations; it has been shown that varying the temporal shape affects laser evolution and can lead to further power amplification [24].

At the dephasing length, the laser pulse in both configurations is compressed, leading to power amplification and renewed bubble expansion [24]. This causes further injection [see Fig. 3(a)], but this high charge beam is restricted in maximum energy gain by beam loading [34]. For a small range of parameters at lower density, the overfocusing can happen only once, producing a single narrow-energy-spread accelerated beam, though with reduced charge; as exemplified by Fig. 1(a). In this case, the long interaction length before injection [25] means that acceleration is limited by laser depletion [24]. With no significant wakefield to interact with once accelerated, the narrow-energy-spread feature can be maintained over long propagation lengths.

We note that our approach to maximizing energy gain in LWFA is different to the usual approach, which requires more laser energy to drive a wakefield over longer distances at lower density [12]. By using an overlarge focal spot to delay injection, we are able to access a relatively stable nonlinear wakefield, enabling acceleration of large amounts of charge to high energies in very short distances. This improved acceleration is witnessed by comparison to the energy gain from previous LWFA experiments as a function of laser power [35,36], shown in Fig. 4. Our results are comparable to those using plasma waveguides with similar laser energy, or using self-guiding with much higher laser energy. Additionally, we have been able to produce high currents of relativistic electrons, with beam charges  $Q_{\text{tot}} > 200$  pC in a simulated duration of 33 fs giving a current of  $I \approx 6$  kA, suitable for driving hybrid wakefield setups [85]. Focusing geometry will be an important

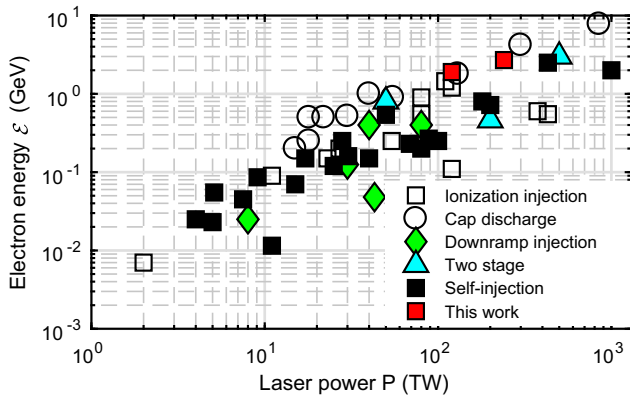


FIG. 4. Scaling of the highest electron energy with laser power for a selection of laser-driven wakefield experiments. Data are from references detailed in Supplemental Material.

consideration for similar experiments to be performed on the many multi-PW laser systems now being developed [86]. Careful choice of focusing would allow these laser systems to fulfil their goals as sources of intense x-ray beams [5,7,13] and ultrashort neutral lepton beams [4,87], and in studies of intense field effects [2,3,88].

We acknowledge funding from STFC (ST/J002062/1, ST/P002021/1, ST/V001639/1) and EPSRC (EP/N027175/1); technical support from the Central Laser Facility; and access to computing facilities from Imperial College Research Computing Service [89].

\*Corresponding author: kristjan.poder@desy.de

†Corresponding author: z.najmudin@imperial.ac.uk

- [1] A. Di Piazza, C. Müller, K. Z. Hatsagortsyan, and C. H. Keitel, *Rev. Mod. Phys.* **84**, 1177 (2012).
- [2] J. M. Cole *et al.*, *Phys. Rev. X* **8**, 011020 (2018).
- [3] K. Poder *et al.*, *Phys. Rev. X* **8**, 031004 (2018).
- [4] G. Sarri, K. Poder, J. M. Cole, W. Schumaker, B. Reville, A. D. Piazza, D. Doria, L. Gizzi, G. Grittani, S. Kar, C. H. Keitel, K. Krushelnick, S. Kushel, S. P. D. Mangles, Z. Najmudin, D. R. Symes, A. G. R. Thomas, M. Vargas, and M. Zepf, *Nat. Commun.* **6**, 1 (2015).
- [5] S. Kneip *et al.*, *Nat. Phys.* **6**, 980 (2010).
- [6] S. Chen, N. D. Powers, I. Ghebregiabher, C. M. Maharjan, C. Liu, G. Golovin, S. Banerjee, J. Zhang, N. Cunningham, A. Moorti, S. Clarke, S. Pozzi, and D. P. Umstadter, *Phys. Rev. Lett.* **110**, 155003 (2013).
- [7] G. Sarri, D. J. Corvan, W. Schumaker, J. M. Cole, A. Di Piazza, H. Ahmed, C. Harvey, C. H. Keitel, K. Krushelnick, S. P. D. Mangles, Z. Najmudin, D. Symes, A. G. R. Thomas, M. Yeung, Z. Zhao, and M. Zepf, *Phys. Rev. Lett.* **113**, 224801 (2014).
- [8] X. Wang *et al.*, *Nat. Commun.* **4**, 1988 (2013).
- [9] H. T. Kim, K. H. Pae, H. J. Cha, I. J. Kim, T. J. Yu, J. H. Sung, S. K. Lee, T. M. Jeong, and J. Lee, *Phys. Rev. Lett.* **111**, 165002 (2013).
- [10] W. P. Leemans, A. J. Gonsalves, H.-S. Mao, K. Nakamura, C. Benedetti, C. B. Schroeder, C. Tóth, J. Daniels, D. E. Mittelberger, S. S. Bulanov, J.-L. Vay, C. G. R. Geddes, and E. Esarey, *Phys. Rev. Lett.* **113**, 245002 (2014).
- [11] H. T. Kim, V. B. Pathak, K. Hong Pae, A. Lifschitz, F. Sylla, J. H. Shin, C. Hojbotá, S. K. Lee, J. H. Sung, H. W. Lee, E. Guillaume, C. Thaury, K. Nakajima, J. Vieira, L. O. Silva, V. Malka, and C. H. Nam, *Sci. Rep.* **7**, 10203 (2017).
- [12] A. J. Gonsalves *et al.*, *Phys. Rev. Lett.* **122**, 084801 (2019).
- [13] J. M. Cole, J. C. Wood, N. C. Lopes, K. Poder, R. L. Abel, S. Alatabi, J. S. J. Bryant, A. Jin, S. Kneip, K. Mecseki, D. R. Symes, S. P. D. Mangles, and Z. Najmudin, *Sci. Rep.* **5**, 13244 (2015).
- [14] J. C. Wood *et al.*, *Sci. Rep.* **8**, 11010 (2018).
- [15] J. M. Cole *et al.*, *Proc. Natl. Acad. Sci. U.S.A.* **115**, 6335 (2018).
- [16] T. Tajima and J. M. Dawson, *Phys. Rev. Lett.* **43**, 267 (1979).
- [17] S. Kneip *et al.*, *Phys. Rev. Lett.* **103**, 035002 (2009).
- [18] J. E. Ralph, C. E. Clayton, F. Albert, B. B. Pollock, S. F. Martins, A. Pak, K. a. Marsh, J. L. Shaw, A. Till, J. P. Palastro, W. Lu, S. H. Glenzer, L. O. Silva, W. B. Mori, C. Joshi, and D. H. Froula, *Phys. Plasmas* **17**, 056709 (2010).
- [19] K. Poder, J. M. Cole, J. C. Wood, N. C. Lopes, S. Alatabi, P. S. Foster, C. Kamperidis, O. Kononenko, C. A. Palmer, D. Rusby, A. Sahai, G. Sarri, D. R. Symes, J. R. Warwick, S. P. D. Mangles, and Z. Najmudin, *Plasma Phys. Controlled Fusion* **60**, 014022 (2018).
- [20] C. E. Max, J. Arons, and A. B. Langdon, *Phys. Rev. Lett.* **33**, 209 (1974).
- [21] G.-Z. Sun, E. Ott, Y. C. Lee, and P. Guzdar, *Phys. Fluids* **30**, 526 (1987).
- [22] W. Lu, M. Tzoufras, C. Joshi, F. S. Tsung, W. B. Mori, J. M. Vieira, R. A. Fonseca, and L. O. Silva, *Phys. Rev. ST Accel. Beams* **10**, 061301 (2007).
- [23] W. Lu, C. Huang, M. Zhou, W. B. Mori, and T. Katsouleas, *Phys. Rev. Lett.* **96**, 165002 (2006).
- [24] M. J. V. Streeter *et al.*, *Phys. Rev. Lett.* **120**, 254801 (2018).
- [25] M. S. Bloom *et al.*, *Phys. Rev. Accel. Beams* **23**, 061301 (2020).
- [26] K. Patorski, *Opt. Lasers Eng.* **8**, 147 (1988).
- [27] C. E. Clayton, J. E. Ralph, F. Albert, R. A. Fonseca, S. H. Glenzer, C. Joshi, W. Lu, K. A. Marsh, S. F. Martins, W. B. Mori, A. Pak, F. S. Tsung, B. B. Pollock, J. S. Ross, L. O. Silva, and D. H. Froula, *Phys. Rev. Lett.* **105**, 105003 (2010).
- [28] B. B. Pollock, C. E. Clayton, L. Divol, S. H. Glenzer, C. Joshi, V. Leurent, K. A. Marsh, A. E. Pak, J. P. Palastro, J. E. Ralph, J. S. Ross, G. R. Tynan, T. Wang, and D. H. Froula, in *Proceedings of PAC09* (2009), pp. 3035–3037, <https://www.osti.gov/biblio/952755>.
- [29] R. Lehe, M. Kirchen, I. A. Andriyash, B. B. Godfrey, and J.-L. Vay, *Comput. Phys. Commun.* **203**, 66 (2016).
- [30] A. Sävert, S. P. D. Mangles, M. Schnell, E. Siminos, J. M. Cole, M. Leier, M. Reuter, M. B. Schwab, M. Möller, K. Poder, O. Jäckel, G. G. Paulus, C. Spielmann, S. Skupin, Z. Najmudin, and M. C. Kaluza, *Phys. Rev. Lett.* **115**, 055002 (2015).
- [31] P. Sprangle, C.-M. Tang, and E. Esarey, *IEEE Trans. Plasma Sci.* **15**, 145 (1987).

- [32] E. Esarey, R. F. Hubbard, W. P. Leemans, A. Ting, and P. Sprangle, *Phys. Rev. Lett.* **79**, 2682 (1997).
- [33] S. S. Bulanov, T. Z. Esirkepov, A. G. R. Thomas, J. K. Koga, and S. V. Bulanov, *Phys. Rev. Lett.* **105**, 220407 (2010).
- [34] M. Tzoufras, W. Lu, F. S. Tsung, C. Huang, W. B. Mori, T. Katsouleas, J. Vieira, R. A. Fonseca, and L. O. Silva, *Phys. Rev. Lett.* **101**, 145002 (2008).
- [35] S. P. D. Mangles, *CERN Yellow Rep.* **1**, 289 (2016).
- [36] See Supplemental Material at <http://link.aps.org/supplemental/10.1103/PhysRevLett.132.195001>, which includes Refs. [37–84], containing the results shown here.
- [37] A. Popp, J. Vieira, J. Osterhoff, Z. Major, R. Hörlein, M. Fuchs, R. Weingartner, T. Rowlands-Rees, M. Marti, R. Fonseca, S. Martins, L. Silva, S. M. Hooker, F. Krausz, F. Grüner, and S. Karsch, *Phys. Rev. Lett.* **105**, 215001 (2010).
- [38] M. Thévenet, D. E. Mittelberger, K. Nakamura, R. Lehe, C. B. Schroeder, J.-L. Vay, E. Esarey, and W. P. Leemans, *Phys. Rev. Accel. Beams* **22**, 071301 (2019).
- [39] D. E. Mittelberger, M. Thévenet, K. Nakamura, A. J. Gonsalves, C. Benedetti, J. Daniels, S. Steinke, R. Lehe, J.-L. Vay, C. B. Schroeder, E. Esarey, and W. P. Leemans, *Phys. Rev. E* **100**, 063208 (2019).
- [40] K. A. Tanaka, T. Yabuuchi, T. Sato, R. Kodama, Y. Kitagawa, T. Takahashi, T. Ikeda, Y. Honda, and S. Okuda, *Rev. Sci. Instrum.* **76**, 13507 (2005).
- [41] K. Zeil, S. D. Kraft, A. Jochmann, F. Kroll, W. Jahr, U. Schramm, L. Karsch, J. Pawelke, B. Hidding, and G. Pretzler, *Rev. Sci. Instrum.* **81**, 013307 (2010).
- [42] K. Poder, Characterisation of self-guided laser wakefield accelerators to multi-GeV energies, Ph.D. thesis, Imperial College London, 2016.
- [43] M. Schnell, A. Sävert, I. Uschmann, O. Jansen, M. C. Kaluza, and C. Spielmann, *J. Plasma Phys.* **81**, 475810401 (2015).
- [44] N. D. Powers, I. Ghebregziabher, G. Golovin, C. Liu, S. Chen, S. Banerjee, J. Zhang, and D. P. Umstadter, *Nat. Photonics* **8**, 28 (2014).
- [45] S. Corde, C. Thaury, A. Lifschitz, G. Lambert, K. Ta Phuoc, X. Davoine, R. Lehe, D. Douillet, A. Rousse, and V. Malka, *Nat. Commun.* **4**, 1501 (2013).
- [46] F. Albert, B. B. Pollock, J. L. Shaw, K. A. Marsh, J. E. Ralph, Y.-H. Chen, D. Alessi, A. Pak, C. E. Clayton, S. H. Glenzer, and C. Joshi, *Phys. Rev. Lett.* **111**, 235004 (2013).
- [47] R. Weingartner, S. Raith, A. Popp, S. Chou, J. Wenz, K. Khrennikov, M. Heigoldt, a. R. Maier, N. Kajumba, M. Fuchs, B. Zeitler, F. Krausz, S. Karsch, and F. Grüner, *Phys. Rev. ST Accel. Beams* **15**, 111302 (2012).
- [48] S. Kneip, C. McGuffey, J. Martins, M. Bloom, V. Chvykov, F. Dollar, R. Fonseca, S. Jolly, G. Kalintchenko, K. Krushelnick, A. Maksimchuk, S. P. D. Mangles, Z. Najmudin, C. A. J. Palmer, K. Phuoc, W. Schumaker, L. Silva, J. Vieira, V. Yanovsky, and A. Thomas, *Phys. Rev. ST Accel. Beams* **15**, 021302 (2012).
- [49] S. Fourmaux, S. Corde, K. T. Phuoc, P. M. Leguay, S. Payeur, P. Lassonde, S. Gnedyuk, G. Lebrun, C. Fourment, V. Malka, S. Sebban, A. Rousse, and J. C. Kieffer, *New J. Phys.* **13**, 033017 (2011).
- [50] D. H. Froula *et al.*, *Phys. Rev. Lett.* **103**, 215006 (2009).
- [51] K. Schmid, L. Veisz, F. Tavella, S. Benavides, R. Tautz, D. Herrmann, A. Buck, B. Hidding, A. Marcinkevicius, U. Schramm, M. Geissler, J. Meyer-ter Vehn, D. Habs, and F. Krausz, *Phys. Rev. Lett.* **102**, 124801 (2009).
- [52] N. A. M. Hafz, T. M. Jeong, I. W. Choi, S. K. Lee, K. H. Pae, V. V. Kulagin, J. H. Sung, T. J. Yu, K.-H. Hong, T. Hosokai, J. R. Cary, D.-K. Ko, and J. Lee, *Nat. Photonics* **2**, 571 (2008).
- [53] S. P. D. Mangles, a. G. R. Thomas, O. Lundh, F. Lindau, M. C. Kaluza, A. Persson, C.-G. Wahlström, K. Krushelnick, and Z. Najmudin, *Phys. Plasmas* **14**, 056702 (2007).
- [54] S. A. Reed, V. Chvykov, G. Kalintchenko, T. Matsuoka, P. Rousseau, V. Yanovsky, C. R. Vane, J. R. Beene, D. Stracener, D. R. Schultz, and A. Maksimchuk, *Appl. Phys. Lett.* **89**, 231107 (2006).
- [55] S. P. D. Mangles, A. G. R. Thomas, M. C. Kaluza, O. Lundh, F. Lindau, A. Persson, F. S. Tsung, Z. Najmudin, W. B. Mori, C. G. Wahlström, and K. Krushelnick, *Phys. Rev. Lett.* **96**, 215001 (2006).
- [56] T. Hosokai, K. Kinoshita, T. Ohkubo, A. Maekawa, M. Uesaka, A. Zhidkov, A. Yamazaki, H. Kotaki, M. Kando, K. Nakajima, S. V. Bulanov, P. Tomassini, A. Giulietti, and D. Giulietti, *Phys. Rev. E* **73**, 036407 (2006).
- [57] B. Hidding, K. U. Amthor, B. Liesfeld, H. Schwoerer, S. Karsch, M. Geissler, L. Veisz, K. Schmid, J. G. Gallacher, S. P. Jamison, D. A. Jaroszynski, G. Pretzler, and R. Sauerbrey, *Phys. Rev. Lett.* **96**, 105004 (2006).
- [58] C.-T. Hsieh, C.-M. Huang, C.-L. Chang, Y.-C. Ho, Y.-S. Chen, J.-Y. Lin, J. Wang, and S.-Y. Chen, *Phys. Rev. Lett.* **96**, 095001 (2006).
- [59] S. Masuda, E. Miura, K. Koyama, M. Adachi, T. Watanabe, S. Kato, and M. Tanimoto, *J. Phys. IV* **133**, 1127 (2006).
- [60] J. Faure, Y. Glinec, A. Pukhov, S. Kiselev, S. Gordienko, E. Lefebvre, J. P. Rousseau, F. Burgy, and V. Malka, *Nature (London)* **431**, 541 (2004).
- [61] S. P. D. Mangles, C. D. Murphy, Z. Najmudin, A. G. R. Thomas, J. L. Collier, A. E. Dangor, E. J. Divall, P. S. Foster, J. G. Gallacher, C. J. Hooker, D. A. Jaroszynski, A. J. Langley, W. B. Mori, P. A. Norreys, F. S. Tsung, R. Viskup, B. R. Walton, and K. Krushelnick, *Nature (London)* **431**, 535 (2004).
- [62] C. G. R. Geddes, C. Toth, J. van Tilborg, E. Esarey, C. B. Schroeder, D. Bruhwiler, C. Nieter, J. Cary, W. P. Leemans, J. van Tilborg, E. Esarey, C. B. Schroeder, D. Bruhwiler, C. Nieter, J. Cary, and W. P. Leemans, *Nature (London)* **431**, 538 (2004).
- [63] S. Kuschel, D. Hollatz, T. Heinemann, O. Karger, M. B. Schwab, D. Ullmann, A. Knetsch, A. Seidel, C. Rödel, M. Yeung, M. Leier, A. Blinne, H. Ding, T. Kurz, D. J. Corvan, A. Sävert, S. Karsch, M. C. Kaluza, B. Hidding, and M. Zepf, *Phys. Rev. Accel. Beams* **19**, 071301 (2016).
- [64] S. Steinke, J. van Tilborg, C. Benedetti, C. G. R. Geddes, C. B. Schroeder, J. Daniels, K. K. Swanson, A. J. Gonsalves, K. Nakamura, N. H. Matlis, B. H. Shaw, E. Esarey, and W. P. Leemans, *Nature (London)* **530**, 190 (2016).
- [65] M. Mirzaie, S. Li, M. Zeng, N. A. M. Hafz, M. Chen, G. Y. Li, Q. J. Zhu, H. Liao, T. Sokollik, F. Liu, Y. Y. Ma, L. Chen, Z. M. Sheng, and J. Zhang, *Sci. Rep.* **5**, 14659 (2015).
- [66] G. Sarri, W. Schumaker, A. Di Piazza, M. Vargas, B. Dromey, M. E. Dieckmann, V. Chvykov, A. Maksimchuk,

- V. Yanovsky, Z.-H. He, B. X. Hou, J. A. Nees, A. G. R. Thomas, C. H. Keitel, M. Zepf, and K. Krushelnick, *Phys. Rev. Lett.* **110**, 255002 (2013).
- [67] M. Z. Mo, A. Ali, S. Fourmaux, P. Lassonde, J. C. Kieffer, and R. Fedosejevs, *Appl. Phys. Lett.* **102**, 134102 (2013).
- [68] M. Z. Mo, A. Ali, S. Fourmaux, P. Lassonde, J. C. Kieffer, and R. Fedosejevs, *Appl. Phys. Lett.* **100**, 074101 (2012).
- [69] C. McGuffey, A. G. R. Thomas, W. Schumaker, T. Matsuoka, V. Chvykov, F. J. Dollar, G. Kalintchenko, V. Yanovsky, A. Maksimchuk, K. Krushelnick, V. Y. Bychenkov, I. V. Glazyrin, and A. V. Karpeev, *Phys. Rev. Lett.* **104**, 025004 (2010).
- [70] A. Pak, K. A. Marsh, S. F. Martins, W. Lu, W. B. Mori, and C. Joshi, *Phys. Rev. Lett.* **104**, 025003 (2010).
- [71] E. Miura, K. Koyama, S. Kato, N. Saito, M. Adachi, Y. Kawada, M. Tanimoto, E. Miura, K. Koyama, S. Kato, and N. Saito, *Appl. Phys. Lett.* **86**, 251501 (2005).
- [72] K. Khrennikov, J. Wenz, A. Buck, J. Xu, M. Heigoldt, L. Veisz, and S. Karsch, *Phys. Rev. Lett.* **114**, 195003 (2015).
- [73] S. Fourmaux, K. Ta Phuoc, P. Lassonde, S. Corde, G. Lebrun, V. Malka, A. Rousse, and J. C. Kieffer, *Appl. Phys. Lett.* **101**, 111106 (2012).
- [74] P. Brijesh, C. Thaury, K. T. Phuoc, S. Corde, G. Lambert, V. Malka, S. P. D. Mangles, M. Bloom, and S. Kneip, *Phys. Plasmas* **19**, 063104 (2012).
- [75] A. J. Gonsalves, K. Nakamura, C. Lin, D. Panasenko, S. Shiraishi, T. Sokollik, C. Benedetti, C. B. Schroeder, C. G. R. Geddes, J. van Tilborg, J. Osterhoff, E. Esarey, C. Toth, and W. P. Leemans, *Nat. Phys.* **7**, 862 (2011).
- [76] K. Schmid, A. Buck, C. M. S. Sears, J. M. Mikhailova, R. Tautz, D. Herrmann, M. Geissler, F. Krausz, and L. Veisz, *Phys. Rev. ST Accel. Beams* **13**, 091301 (2010).
- [77] B. B. Pollock, C. E. Clayton, J. E. Ralph, F. Albert, A. Davidson, L. Divol, C. Filip, S. H. Glenzer, K. Herpoldt, W. Lu, K. a. Marsh, J. Meinecke, W. B. Mori, A. Pak, T. C. Rensink, J. S. Ross, J. Shaw, G. R. Tynan, C. Joshi, and D. H. Froula, *Phys. Rev. Lett.* **107**, 045001 (2011).
- [78] J. S. Liu, C. Q. Xia, W. T. Wang, H. Y. Lu, C. Wang, a. H. Deng, W. T. Li, H. Zhang, X. Y. Liang, Y. X. Leng, X. M. Lu, C. Wang, J. Z. Wang, K. Nakajima, R. X. Li, and Z. Z. Xu, *Phys. Rev. Lett.* **107**, 035001 (2011).
- [79] P. A. Walker, N. Bourgeois, W. Rittershofer, J. Cowley, N. Kajumba, a. R. Maier, J. Wenz, C. M. Werle, S. Karsch, F. Grüner, D. R. Symes, P. P. Rajeev, S. J. Hawkes, O. Chekhlov, C. J. Hooker, B. Parry, Y. Tang, and S. M. Hooker, *New J. Phys.* **15**, 045024 (2013).
- [80] H. Lu, M. Liu, W. Wang, C. Wang, J. Liu, A. Deng, J. Xu, C. Xia, W. Li, H. Zhang, X. Lu, J. Wang, X. Liang, Y. Leng, B. Shen, K. Nakajima, R. Li, and Z. Xu, *Appl. Phys. Lett.* **99**, 091502 (2011).
- [81] T. P. A. Ibbotson *et al.*, *Phys. Rev. ST Accel. Beams* **13**, 031301 (2010).
- [82] T. P. Rowlands-Rees, C. Kamperidis, S. Kneip, a. J. Gonsalves, S. P. D. Mangles, J. G. Gallacher, E. Brunetti, T. P. A. Ibbotson, C. D. Murphy, P. S. Foster, M. J. V. Streeter, F. Budde, P. a. Norreys, D. a. Jaroszynski, K. Krushelnick, Z. Najmudin, and S. M. Hooker, *Phys. Rev. Lett.* **100**, 105005 (2008).
- [83] S. Karsch, J. Osterhoff, A. Popp, T. P. Rowlands-Rees, Z. S. Major, M. Fuchs, B. Marx, R. Hölein, K. Schmid, L. Veisz, S. Becker, U. Schramm, B. Hidding, G. Pretzler, D. Habs, F. Grüner, F. Krausz, and S. M. Hooker, *New J. Phys.* **9**, 415 (2007).
- [84] W. P. Leemans, B. Nagler, A. J. Gonsalves, C. Tóth, K. Nakamura, C. G. R. Geddes, E. Esarey, C. B. Schroeder, and S. M. Hooker, *Nat. Phys.* **2**, 696 (2006).
- [85] A. Martinez de la Ossa *et al.*, *Phil. Trans. R. Soc. A* **377**, 20180175 (2019).
- [86] C. Danson, D. Hillier, N. Hopps, and D. Neely, *High Power Laser Sci. Eng.* **3**, e3 (2015).
- [87] J. Warwick *et al.*, *Phys. Rev. Lett.* **119**, 185002 (2017).
- [88] O. J. Pike, F. Mackenroth, E. G. Hill, and S. J. Rose, *Nat. Photonics* **2**, 1 (2014).
- [89] Imperial college research computing service, <http://dx.doi.org/10.14469/hpc/2232>.